

-
- Rock mass qualities are based on the summary results from the 1998 and 2003 core logging and strength testing exercises. The metasediments identified at the deposit will comprise the back, sidewalls, and hanging wall of all stopes. Approximately 660 m of logged metasediment core was compiled to perform a statistical rock mass classification. Statistical results for the parameters required are summarized in Figure 1.
 - Rock mass classification was carried using the NGI Q-system parameter designations after Barton 1974. The results are presented in Figure 1 and consider a mean and range of values based on ± 1 standard deviation.
 - The quality of rock masses can be classified as fair ($3 \leq Q' \leq 10$) for the -1 std case and good ($10 \leq Q' \leq 40$) for the mean and +1 std case. As the major controlling factor within the ratings for the rock mass classification is the strength of the rock unit, the metasediments can be generally simplified as strong ($50\text{MPa} < \text{UCS} < 100 \text{MPa}$) with a uniaxial compressive strength of 75 MPa.
 - The in-situ stress conditions were estimated at two depths (100m and 250m) using Herget's equations (Reference 2). Herget's equations were developed by analysis of compiled data that considers the general trends and broad geological categories of rock stresses in the Canadian Shield. These in-situ stress conditions were subsequently applied to a 3D modelling program, Examine3D. The model assumed a single opening and nominal stope dimensions with a height of 25m, a traverse span of 20m, a strike span of 20 m, and a stope inclination of 50 degrees. The induced stresses were calculated at the mid points of the back, the side wall, and the hanging wall (Refer to Figures 2 and 3).
 - Critical discontinuity set orientations were extracted from the summary stereonet produced from the oriented core and surface mapping program. The peak orientations of the discontinuity sets are included as Figure 4.
 - Based on the parameters described above, the Mathews/Potvin stability factors A, B, and C were chosen (see Reference 1). A summary of input parameters and the resulting Stability Numbers are presented in Table 1.
 - For the range of rock qualities found for the metasediments a Stability Number (N') was calculated and potential shape factors determined for the maximum unsupported stable case and mean unsupported transition case for stope backs, sidewalls and hangingwalls at both 100 m and 250 m depth.

Results of the analysis have been plotted for stope back, stope hanging wall, and stope side wall as shown in Figures 5 to 10. The considerations for opening sizes have been based on back and sidewall stabilities as they will dictate the stope dimensions. The stope back is anticipated to be the major limiting factor on stope dimensioning due to induced stress and potential gravity falls and slabbing.

Plotted also within the Mathews analysis graphs in Figures 5 through 10 are the Equivalent Linear Overbreak/Slough (ELOS) dilution contours, using an empirical technique proposed by Clark and Pakalnis (1997 – Reference 3). ELOS is equivalent to the average depth of overbreak

or sloughage measured relative to the planned (drilled-off) stope boundary. Stope surfaces with $ELOS \leq 0.5$ m are considered stable, whereas caving is assumed to occur for $ELOS > 5$ m. The volume of rock and, consequently, the potential dilution can be estimated by multiplying the ELOS numbers by the area of the analyzed stope surface. The potential overbreak for a stope side wall, for example, with a span of 15 m, a height of 25 m and an estimated ELOS of 1 m would be about 375 m^3 . The potential dilution can then be estimated by dividing this overbreak volume by the total stope volume.

In order to assist in the selection of optional stoping dimensions, a series of graphs have been presented in Figures 11 through 16 which allow the long span and short span of stope walls to be determined based on the permissible shape factor (hydraulic radius = area/perimeter). The shape factors considered for the metasediments are:

- 1) the intersection of the stability number (N') with the stable zone / unsupported transition zone curve, corresponding to the maximum sized unsupported opening considered to be "stable" (ie. minimum dilution), and,
- 2) the mid point within the unsupported transition zone of the Mathews chart. This corresponds to a shape factor that is the average maximum sized opening that lies in the transition between no support required and support required.

Table 2 presents an example of a range of maximum recommended stope geometries based on possible excavated conditions. The example considers the calculated hydraulic radii for the mean stable, and the mean unsupported transition cases. The allowable strike span and sublevel height were determined by varying the transverse spans at 15, 30, and 45 meters respectively, based on the following assumptions and logic:

- The stope back is excavated to the maximum strike span to achieve stability.
- The sidewall is more sensitive than the hanging wall to increased opening size, therefore the sidewall shape factor is used to calculate sublevel height.

TABLE 2 - EXAMPLES OF POTENTIAL STOPE DIMENSIONS

Depth Below Ground Surface	HYDRAULIC RADIUS BASED UPON ⁺	TRANSVERSE SPAN (m)				TRANSVERSE SPAN (m)			
		HR (m)	15	30	45	HR (m)	15	30	45
			STRIKE SPAN (m)				SUBLEVEL HEIGHT (m)		
100 m	Stable (mean) Case	4.3	20.2	12.1	10.6	6.8	100 ⁺	24.9	12.4
	Unsupported Transition (mean) Case	5.5	41.3	17.4	14.6	8.1	100 ⁺	35.2	25.3
250 m	Stable (mean) Case	3.9	16.3	10.5	9.4	5.4	38.6	16.9	14.2
	Unsupported Transition (mean) Case	5.1	31.9	15.5	13.2	6.7	100 ⁺	24.2	19.1

* Limited to 100m based on practical considerations.

+ For the value of hydraulic radius used for each case please refer to Table 1. For example, the hydraulic radius for the stope back was used to calculate the strike span, whereas the hydraulic radius for the sidewalls was used to calculate the sublevel height. Colour coded for use with Table 1.

Based on results of the Stability Method analysis for stope stability, the following observations are made:

- For a transverse mining method employing 15m wide stopes and 25m high sub-levels, and assuming an average rock mass quality:
 - Transverse stoping distances of up to 20 m length at 100m depth and 16m at 250m depth should be achievable with a “stable” back resulting over the short term. An estimated ELOS of 0.6m in the back, 0.5m in the sidewalls and <0.5m in the hangingwall/footwall would result.
 - At transverse stoping distances of between 20 and 40m transverse length at 100m depth and between 16 and 32m transverse length at 250m depth, the stability of the stope back falls into the “transition” region between stable and requiring support for excavation stability over the short term. An estimated ELOS of 1.3m in the back, 0.8m in the sidewalls and <0.5m in the hangingwall/footwall would result.
 - At transverse stoping distances greater than 40m transverse length at 100m depth and 32m at 250m depth, the stability of the stope back falls into the zone where support will be required for stability over the short term. An estimated ELOS of 1m in the back, 1.0m in the sidewalls and <0.5m in the hangingwall/footwall would result.
 - At transverse stoping distances greater than 80m transverse length at 100m depth and 45m at 250m depth, the stability of the stope sidewalls falls into the zone where support will be required for stability over the short term. An estimated ELOS of 1.5m in the sidewalls would result.

- Although the stope backs plot in the “stable” zone for transverse distances up to 20m, this refers to short term stability, or that achievable directly after a blast and for a few months thereafter. In the case of blasthole stoping the overcut of an underlying stope will become the overcut of the next sequential stope and may be open for many months during drilling, mucking and backfilling stages. For this reason back support will be required for this longer term stability to achieve a safe working environment.
- It is recommended that at a feasibility level of design, primary support of the stope overcuts employ a bolting pattern of 2.4 m long rebar on a 2m by 2m pattern with 4x4 (100mm x 100mm) weld mesh screen.
- It is also recommended that a cable bolting pattern employing 5m long bolts on a 2m x 2m pattern be planned for the stope backs.

It should be noted that these empirical recommendations are based on a simple mining geometry. Once a mining plan incorporating the proposed mining sequence has been established, the recommendations should be reviewed to incorporate potential influence of the mine plan and changing stress concentrations on the initial recommendations.

We trust that the above information regarding possible stope dimensioning and preliminary support recommendations is sufficient for your current requirements. If you require any additional information, please contact our office.

Sincerely,

GOLDER ASSOCIATES LTD.

Original signed by:

Chris Sharpe, B. Eng

Original signed by:

C.M. Steed, P.Eng
Principal

CAS/CMS/ms

n:\active\2003\1117\03-1117-029 fortune minerals\stope dimensions aug 2004\technical memorandum-stoping dimensionv3.doc

REFERENCES

1 – Hoek, E, Kaiser, P.K, and Bawden, W.F. Support of Underground Excavations in Hard Rock, Chapter 14 – The Stability Graph Method. A.A. Balkema, 1995.

2 - Herget, G. Rock stresses and rock stress monitoring in Canada. MRL 90-011(TR) December 1990.

3 – Clark, L.M. and Pakanis, R.C. (1997). An empirical design approach for estimating unplanned dilution from open-stope hanging walls and footwalls. Proc 99th CIM Annual General Meeting, Vancouver.

**TABLE 1
SUMMARY OF MATHEWS STABILITY ANALYSIS INPUT PARAMETERS
AND RESULTING HYDRALIC RADIUS**

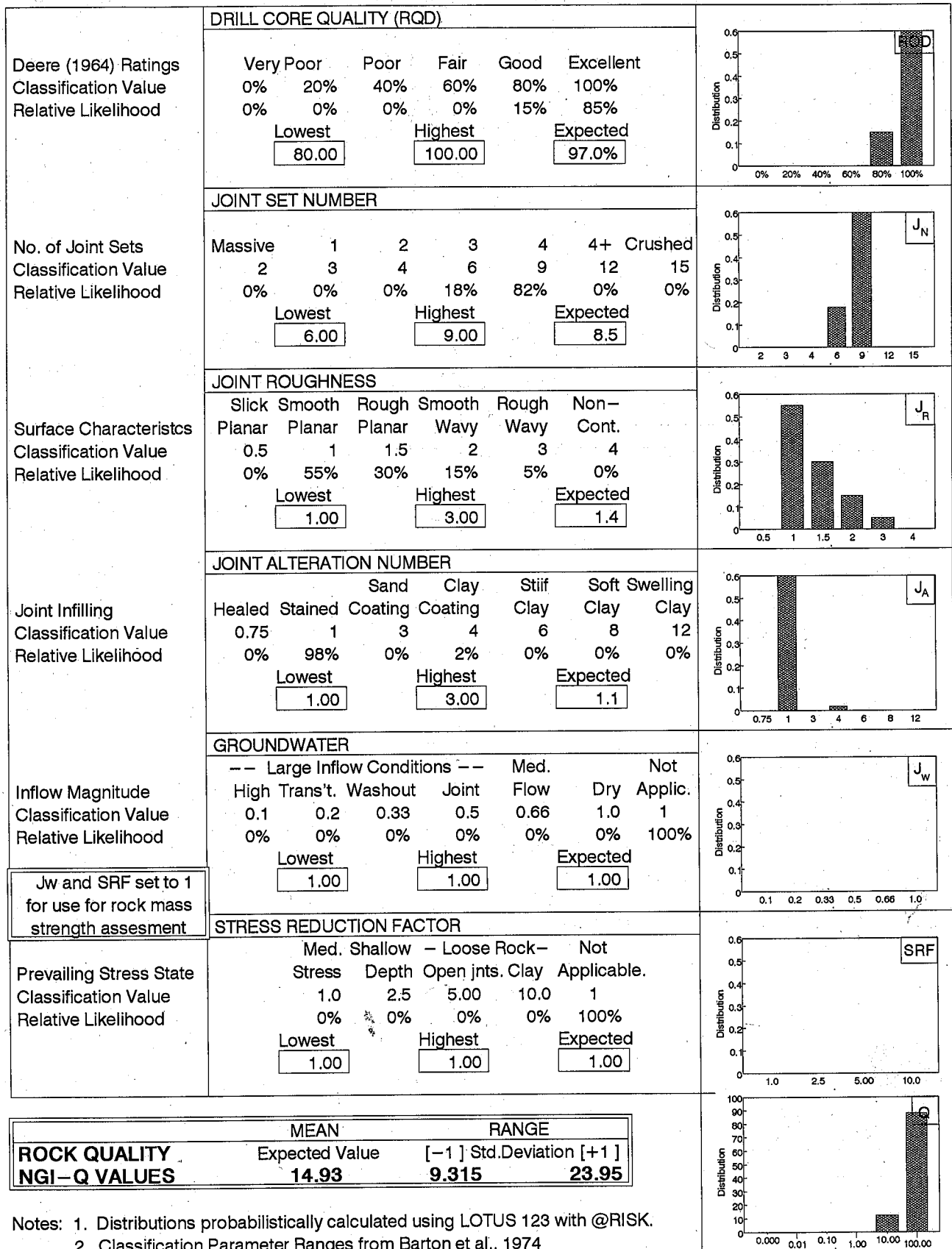
Rock Type	Q'	A	B	C	Calculated N'	HYDRAULIC RADIUS	
						MAXIMUM STABLE UNSUPPORTED (m)	AVERAGE UNSUPPORTED TRANSITION (m)
Depth 100 m							
BACK STABILITY							
Metasediments (-1 std.)	9.3	0.25	0.6	2	2.79	3.5	4.7
Metasediments Stable (mean)	14.9	0.25	0.6	2	4.48	4.3	5.5
Metasediments Stable (+1 std.)	24.0	0.25	0.6	2	7.19	5.2	6.4
SIDEWALL STABILITY							
Metasediments (-1 std.)	9.3	0.35	0.55	5	8.97	5.6	6.9
Metasediments Stable (mean)	14.9	0.35	0.55	5	14.37	6.8	8.1
Metasediments Stable (+1 std.)	24.0	0.35	0.55	5	23.05	8.3	9.4
HW STABILITY							
Metasediments (-1 std.)	9.3	1.00	0.3	4	11.18	6.2	7.4
Metasediments Stable (mean)	14.9	1.00	0.3	4	17.92	7.5	8.7
Metasediments Stable (+1 std.)	24.0	1.00	0.3	4	28.74	9.0	10.1
Depth 250 m							
BACK STABILITY							
Metasediments (-1 std.)	9.3	0.20	0.6	2	2.24	3.4	4.4
Metasediments Stable (mean)	14.9	0.20	0.6	2	3.58	3.9	5.1
Metasediments Stable (+1 std.)	24.0	0.20	0.6	2	5.75	4.7	6.0
SIDEWALL STABILITY							
Metasediments (-1 std.)	9.3	0.2	0.55	5	5.12	4.5	5.8
Metasediments Stable (mean)	14.9	0.2	0.55	5	8.21	5.4	6.7
Metasediments Stable (+1 std.)	24.0	0.2	0.55	5	13.17	6.6	7.8
HW STABILITY							
Metasediments (-1 std.)	9.3	1.00	0.3	4	11.18	6.2	7.4
Metasediments Stable (mean)	14.9	1.00	0.3	4	17.92	7.5	8.7
Metasediments Stable (+1 std.)	24.0	1.00	0.3	4	28.74	9.0	10.1

Note: Colour Coded For Use with Table 2

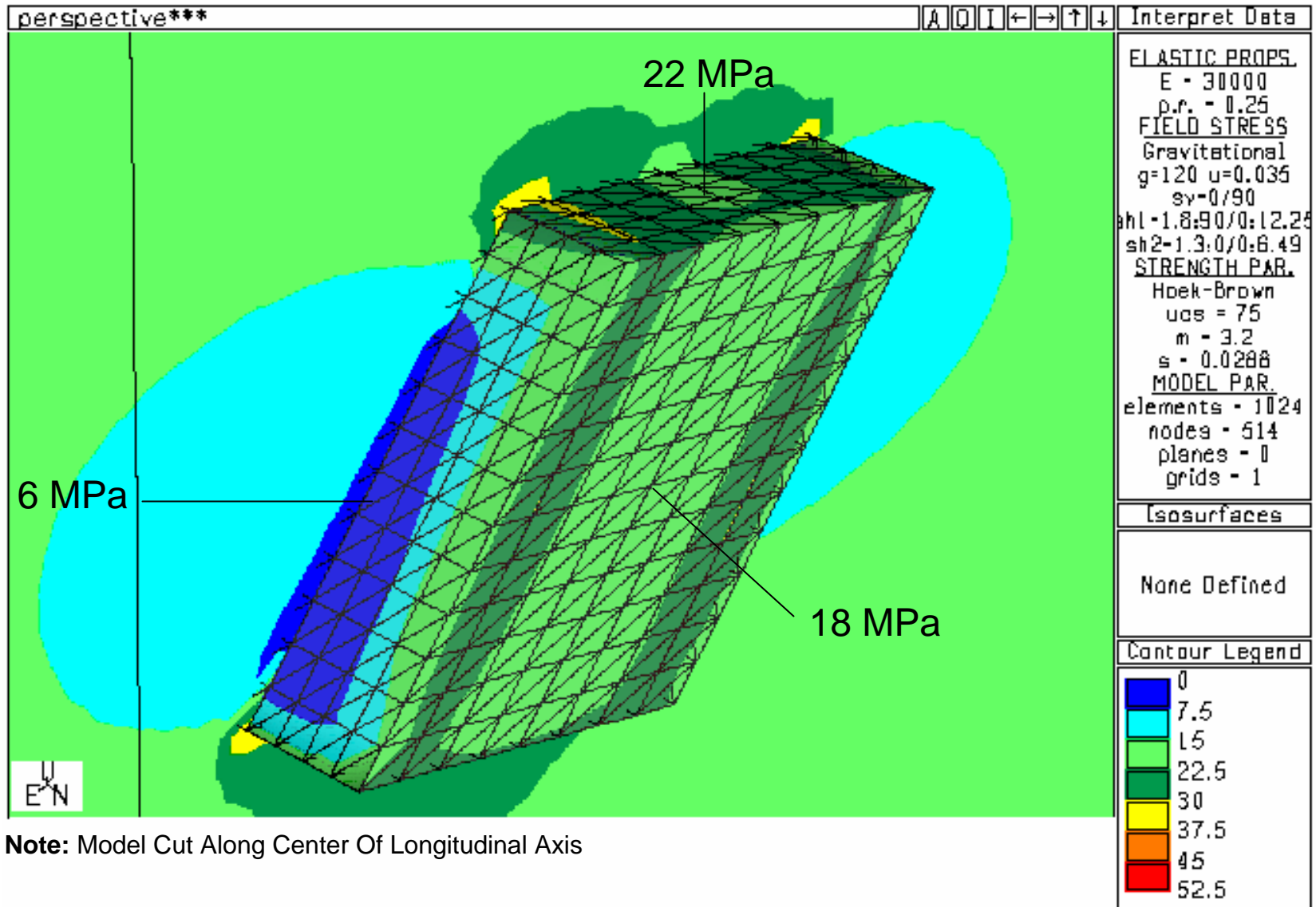
FIGURES

NICO DEPOSIT METASEDIMENTS
NGI – ROCK QUALITY INDEX (Q')
 (Based On Results From 660m Of Logged Metasediment Core)

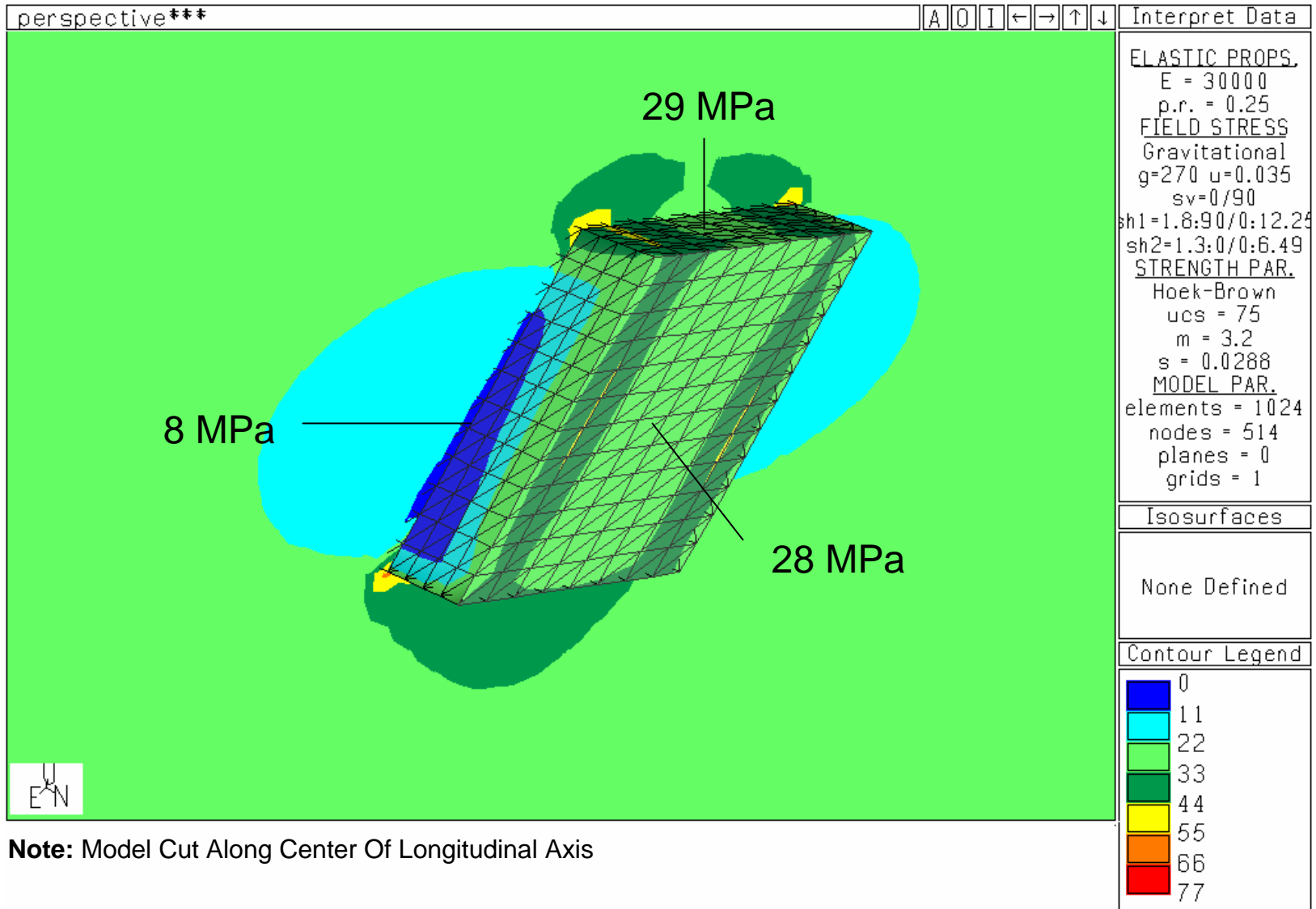
FIGURE 1



Notes: 1. Distributions probabilistically calculated using LOTUS 123 with @RISK.
 2. Classification Parameter Ranges from Barton et al., 1974



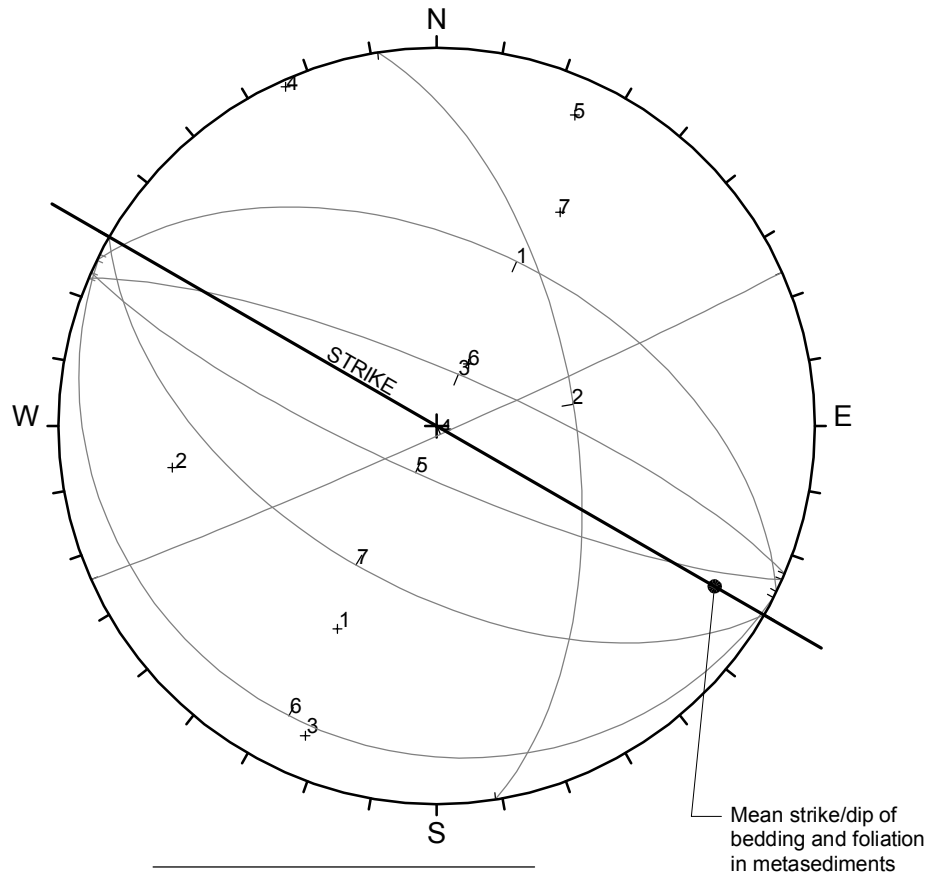
Note: Model Cut Along Center Of Longitudinal Axis



Note: Model Cut Along Center Of Longitudinal Axis

PEAK ORIENTATIONS OF DISCONTINUITY POPULATIONS FROM SURFACE MAPPING AND ORIENTED CORE

FIGURE 4



ORIENTATIONS:

ID	Dip	Direction
1	50	026
2	60	081
3	78	023
4	88	156
5	79	204
6	15	207
7	55	210

NOTES:

Peak Orientations based on review of 1998, 2000 and 2003 stereonets of Oriented core and surface mapping.

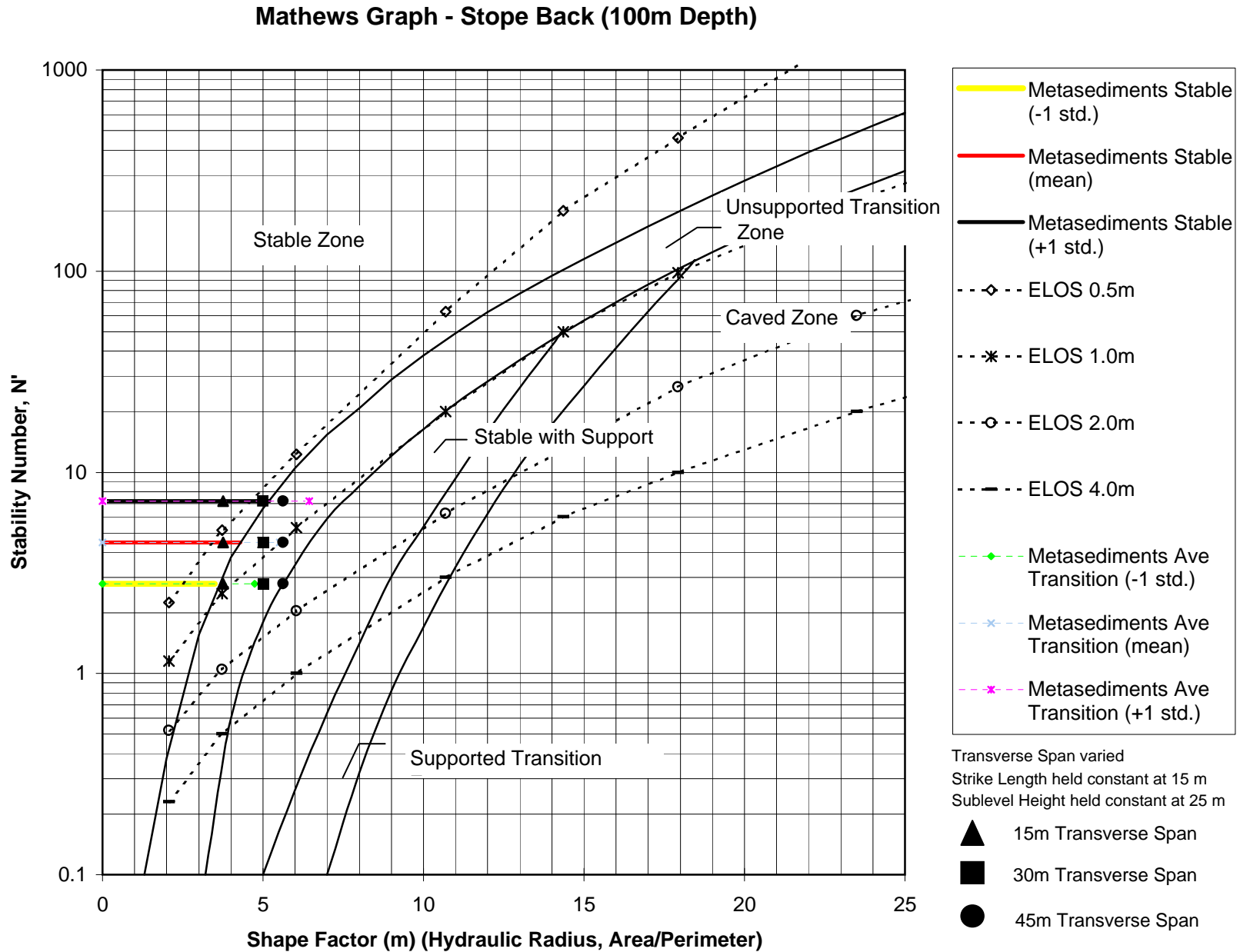
DATE: JANUARY 2005

PROJECT: 03-1117-029

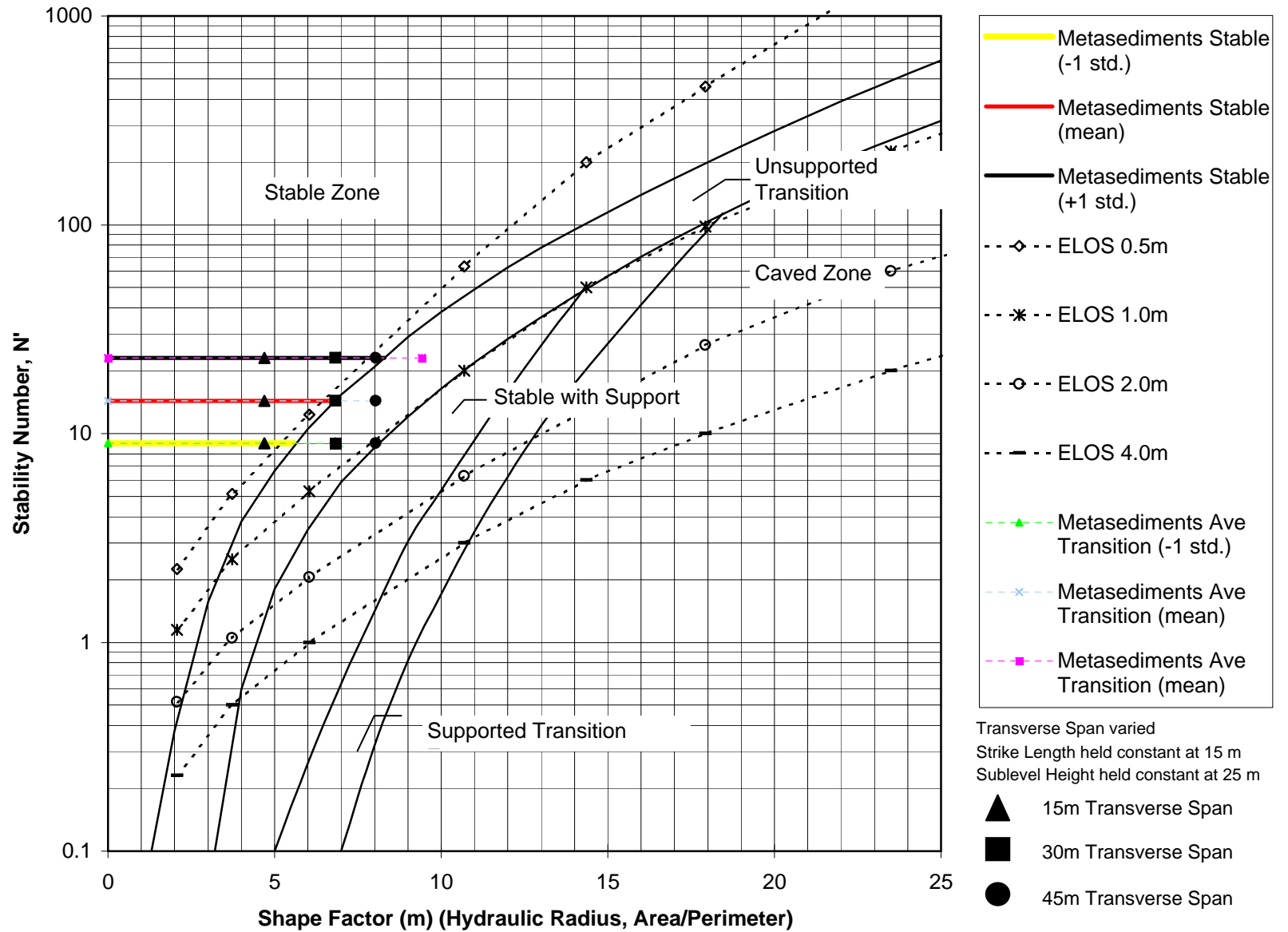


CAD: JDR

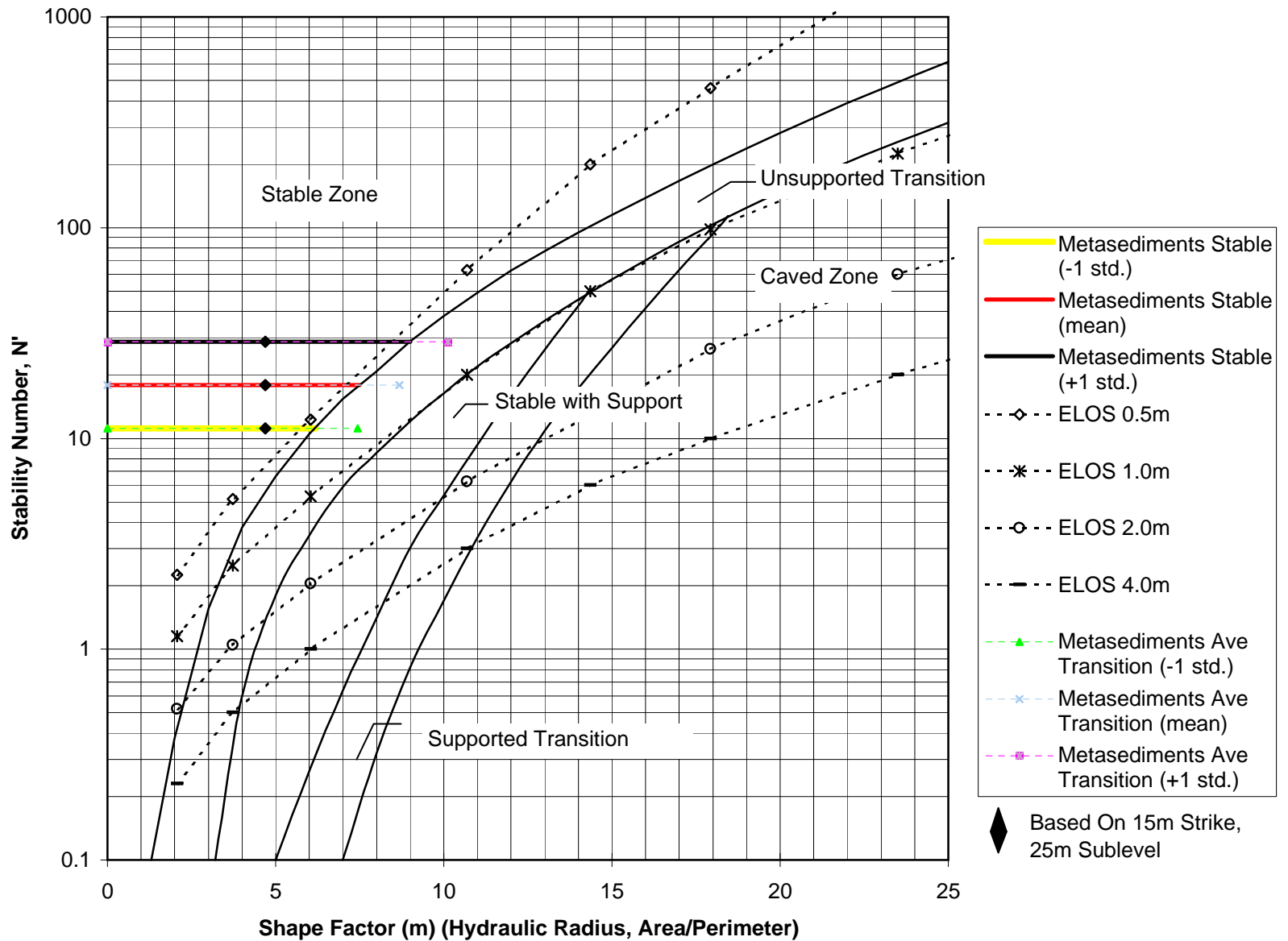
CHK: CAS



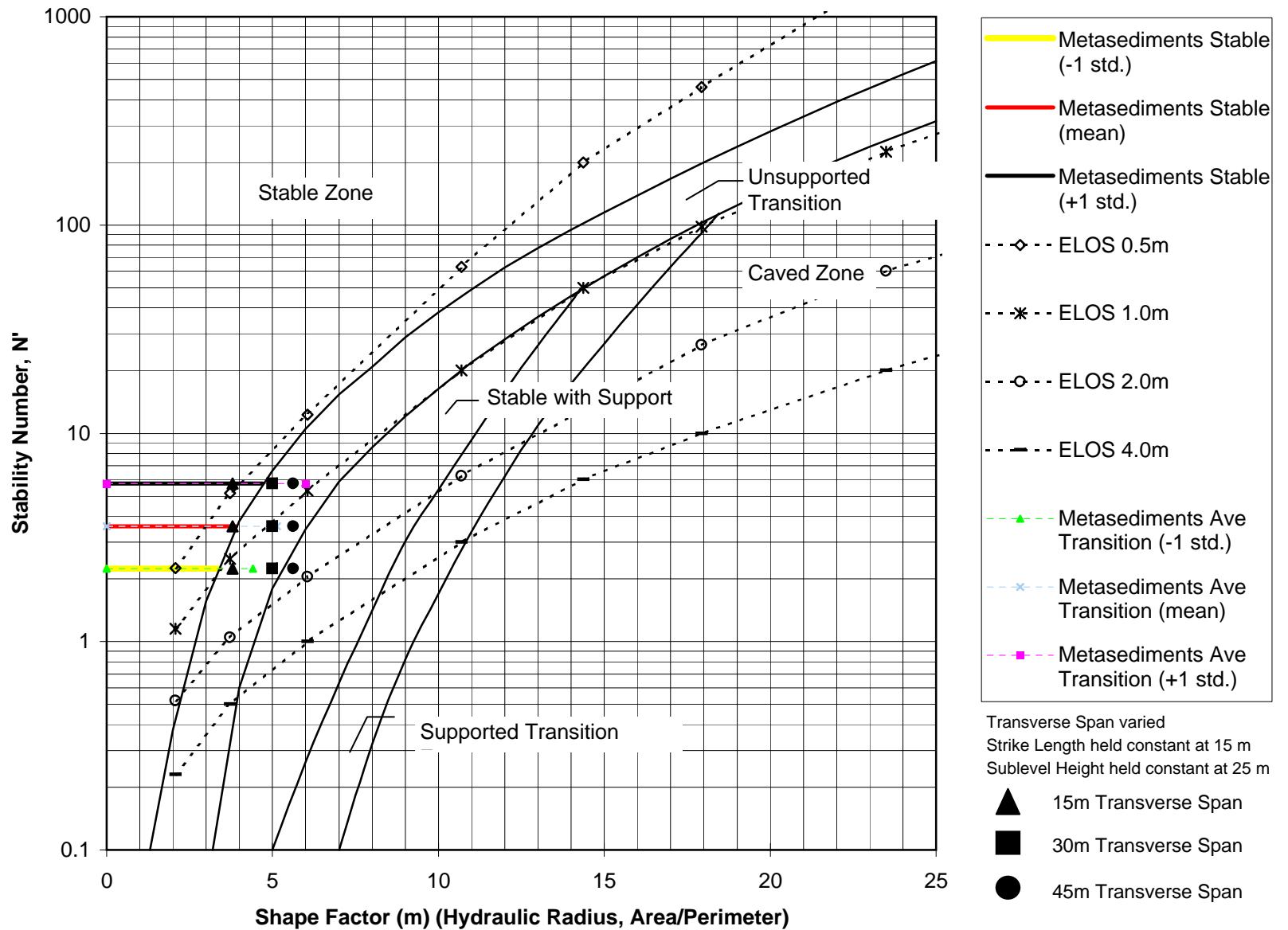
Mathews Graph - Stope SW (100m Depth)



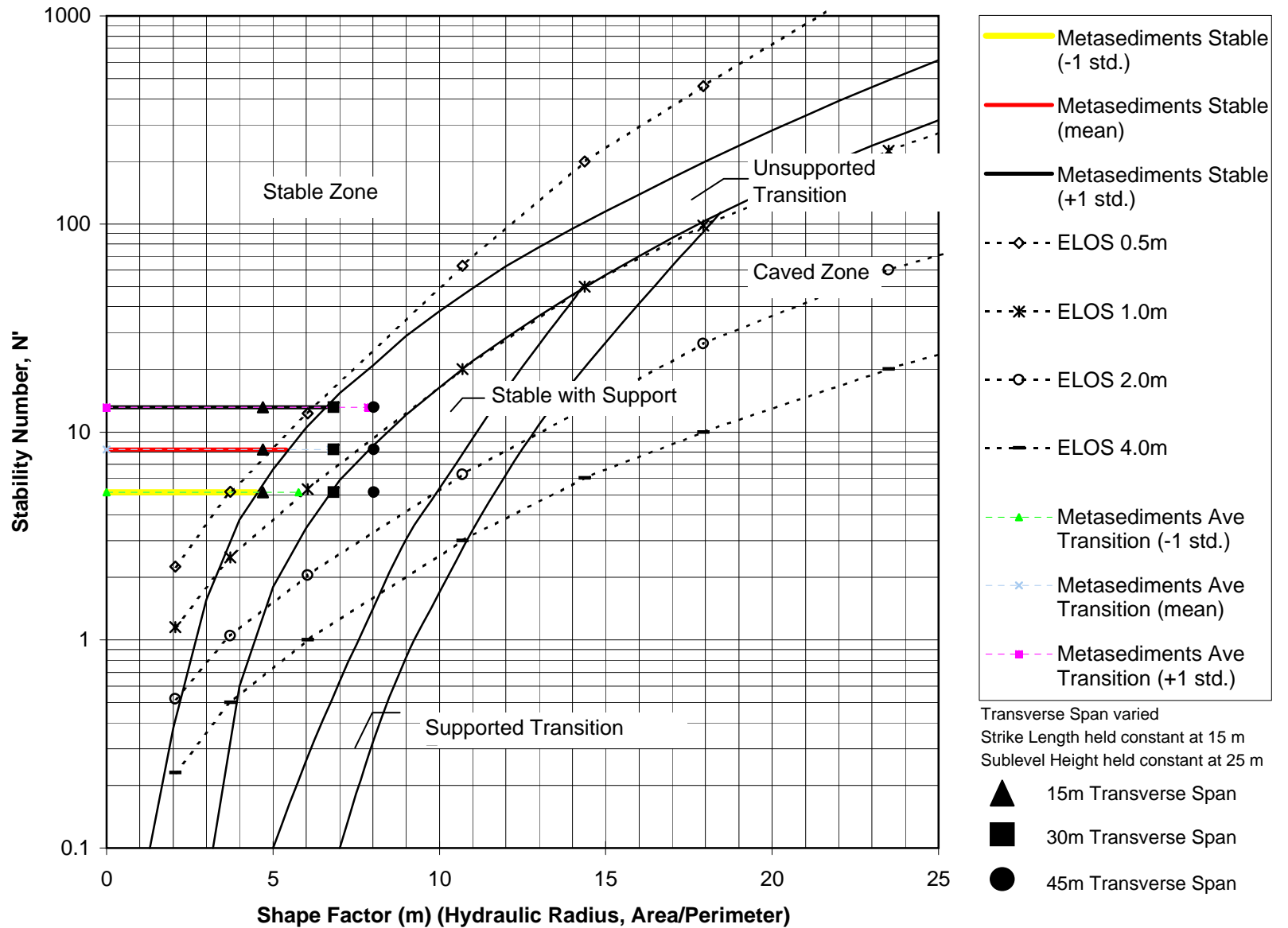
Mathews Graph - Stope HW (100m Depth)



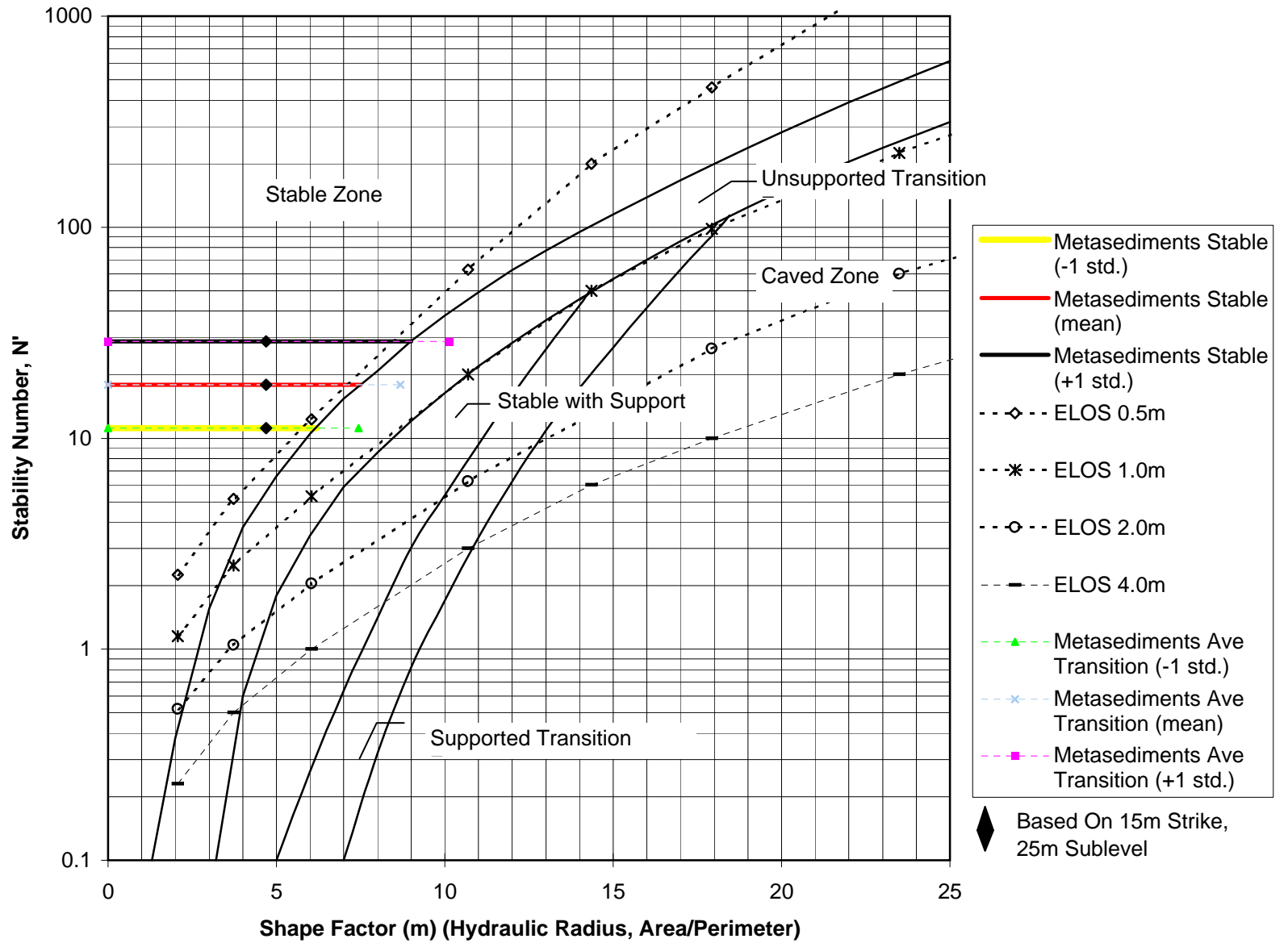
Mathews Graph - Stope Back (250m Depth)



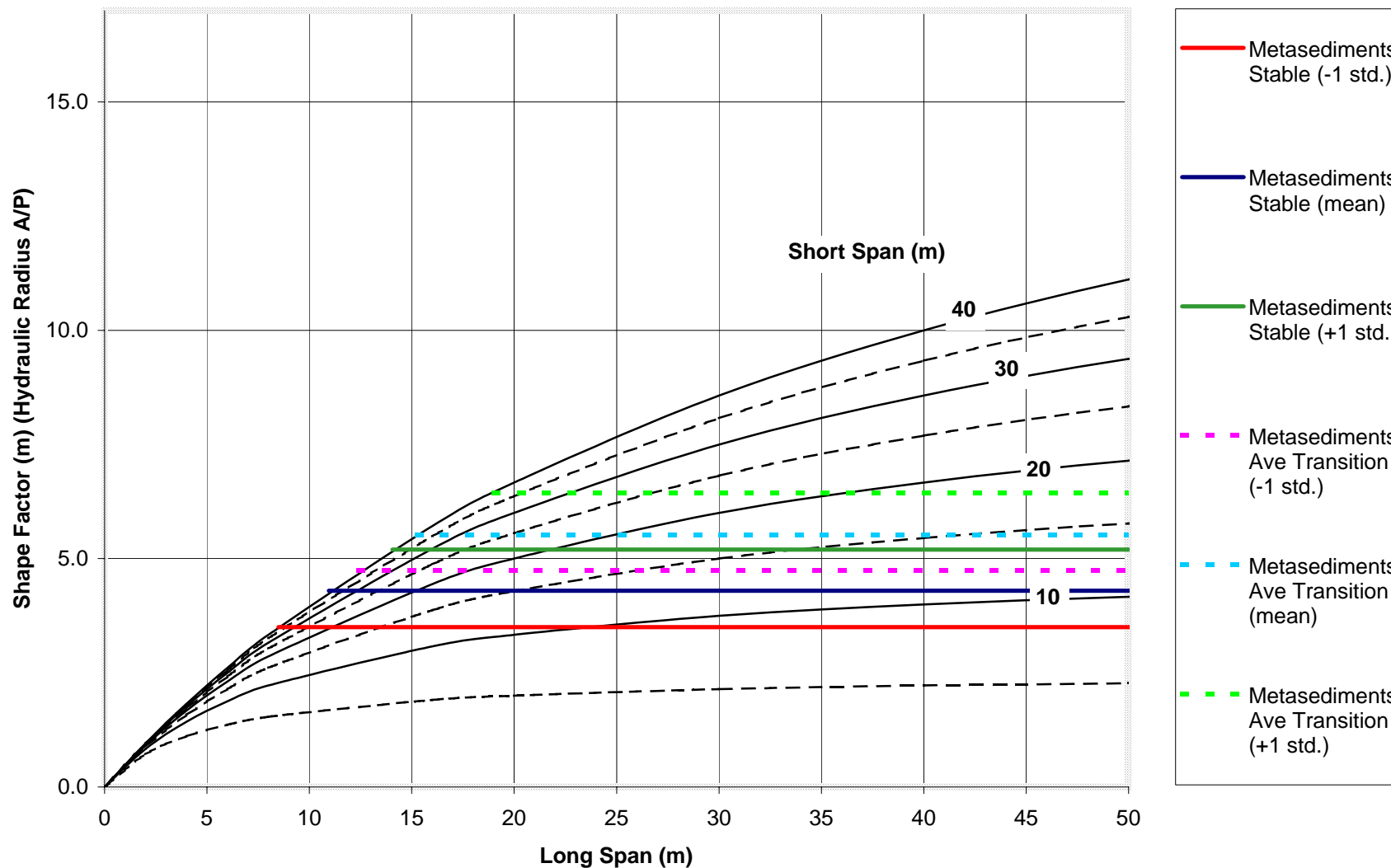
Mathews Graph - Stope SW (250m Depth)



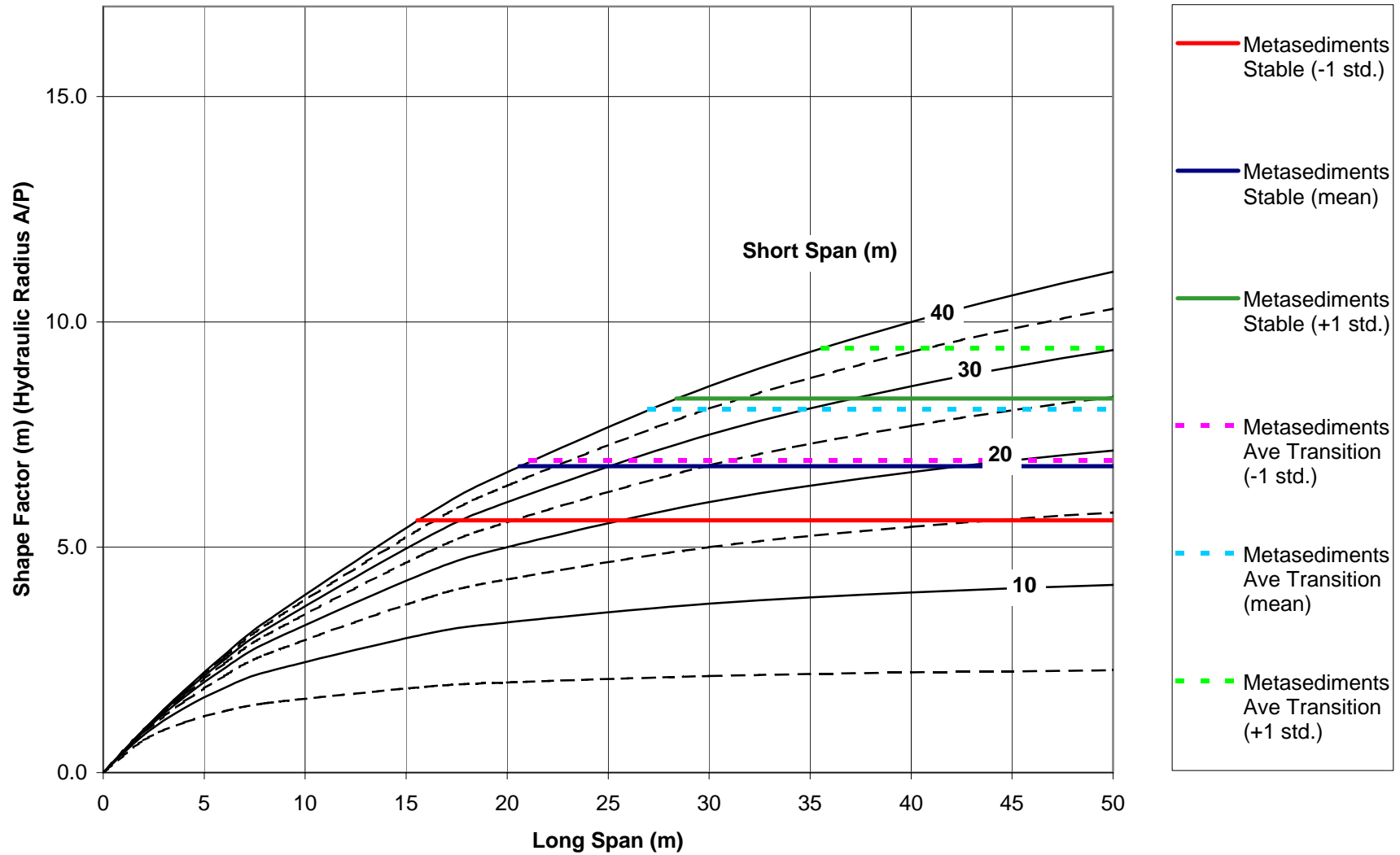
Mathews Graph - Stope HW (250m Depth)



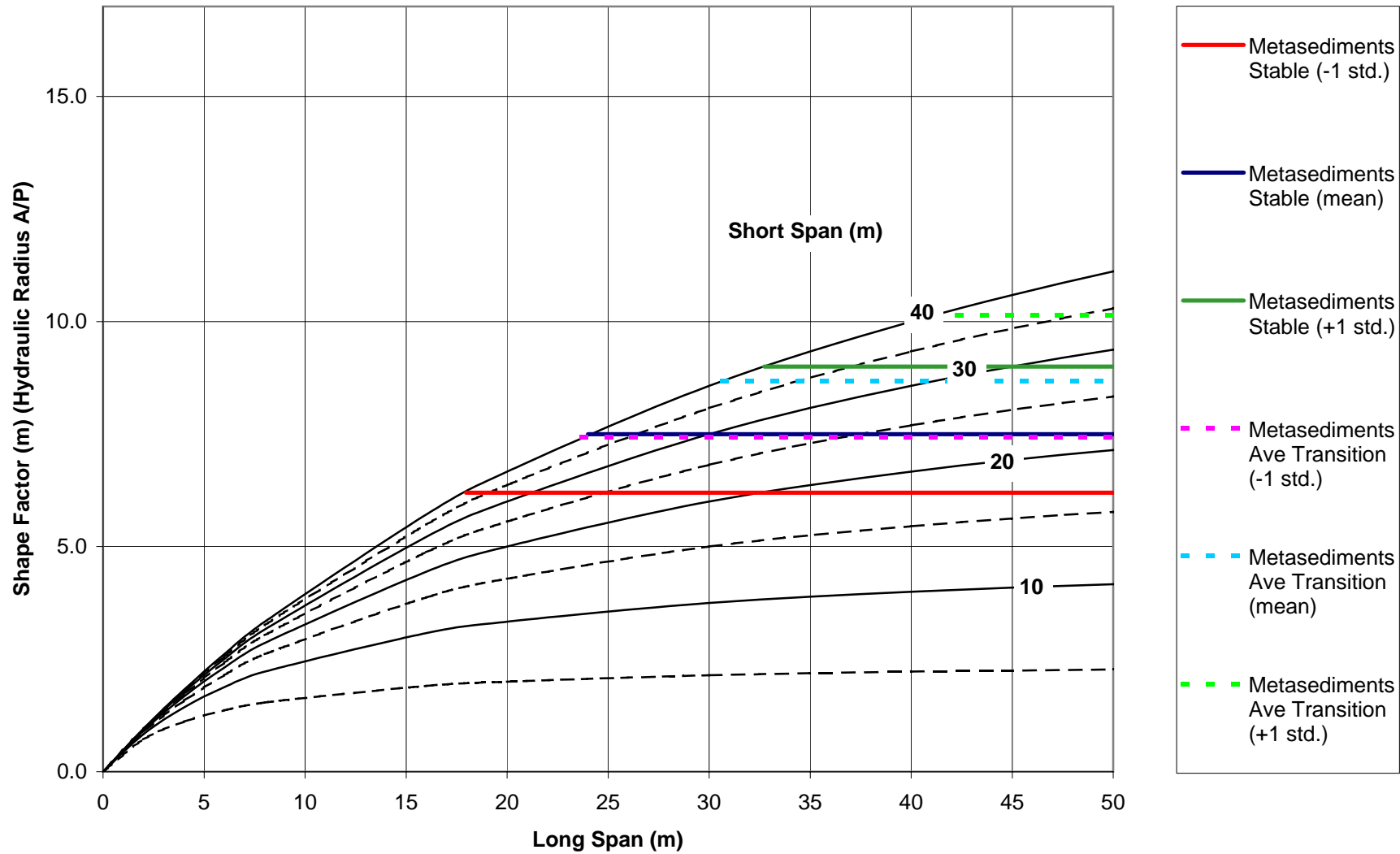
STOPE BACK - Shape Factor Chart (100m Depth)



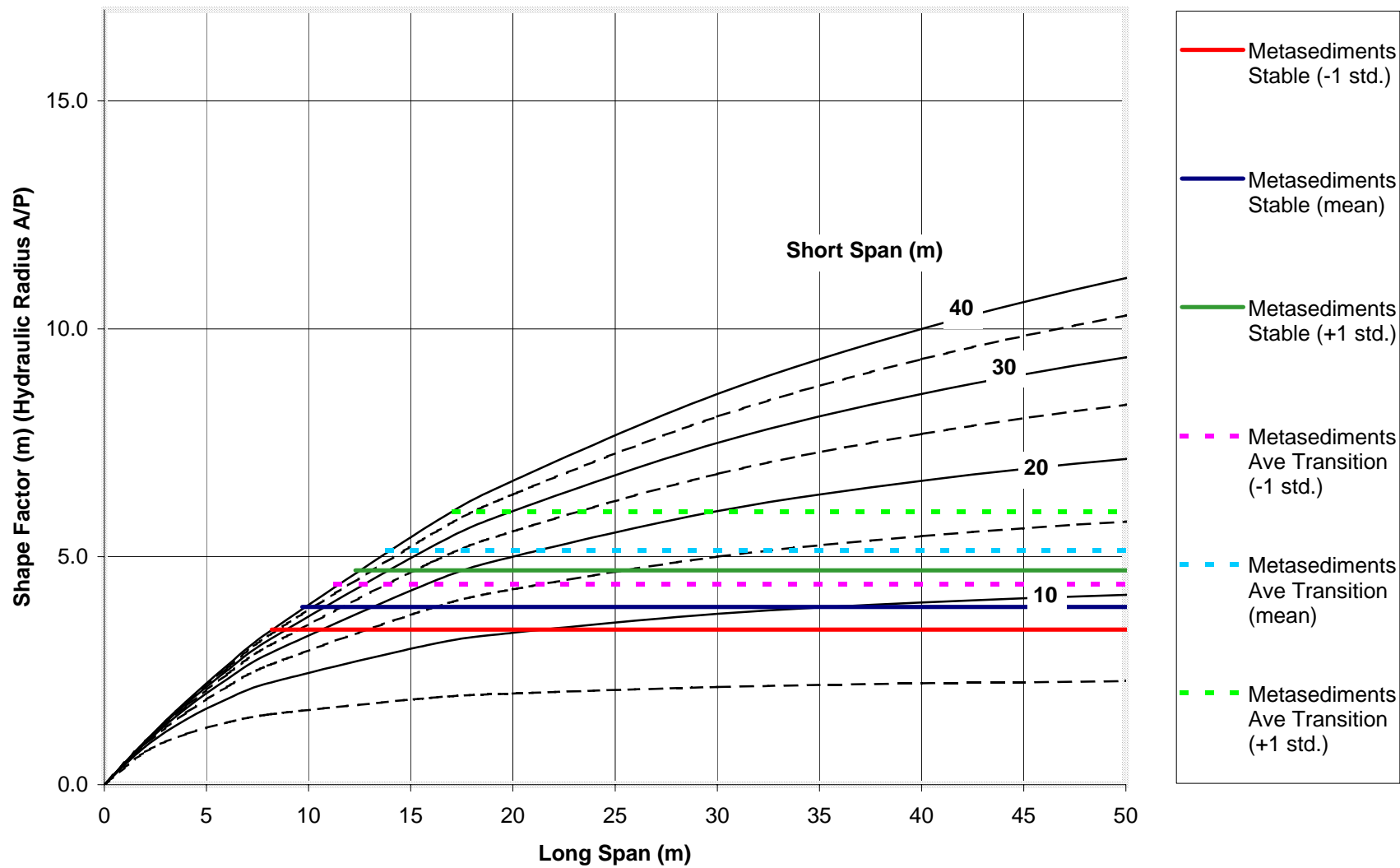
SIDE WALL - Shape Factor Chart (100m Depth)



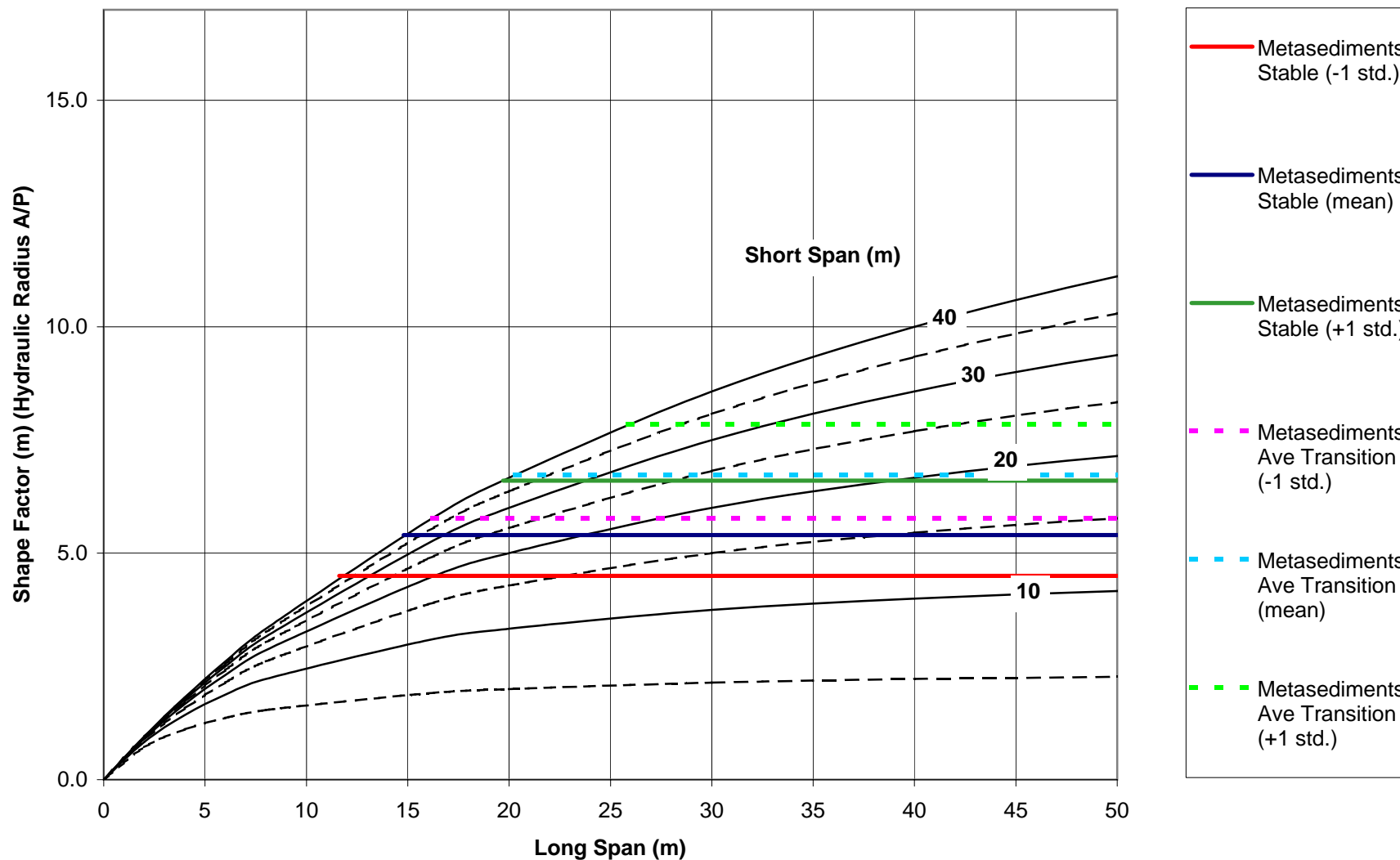
Hanging Wall - Shape Factor Chart (100m Depth)



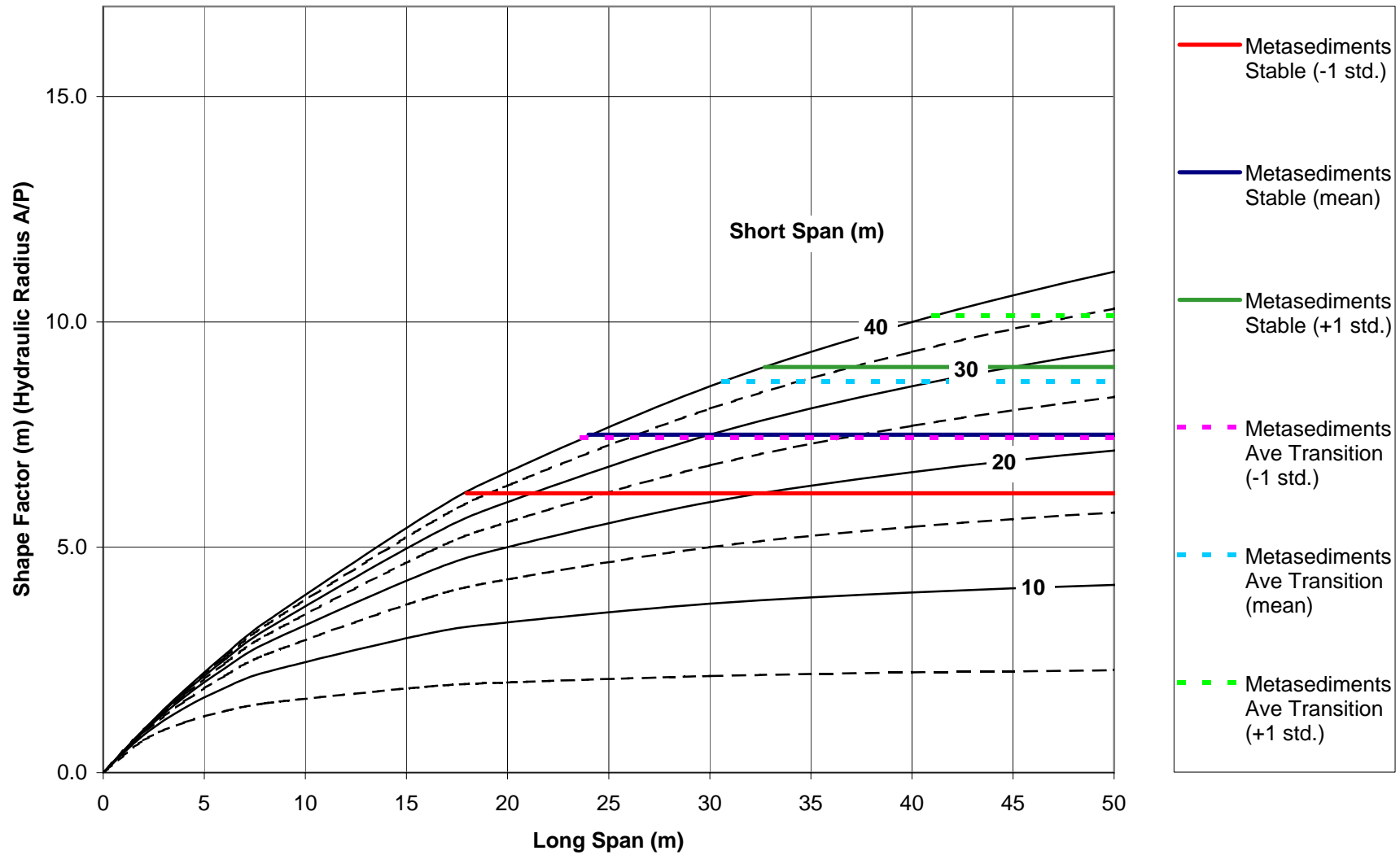
STOPE BACK - Shape Factor Chart (250m Depth)



SIDE WALL - Shape Factor Chart (250m Depth)



Hanging Wall - Shape Factor Chart (250m Depth)



APPENDIX A
MATHEWS METHOD

14 The Stability Graph method

14.1 Introduction

Potvin (1988), Potvin and Milne (1992) and Nickson (1992), following earlier work by Mathews et al. (1981), developed the Stability Graph Method for cablebolt design. The current version of the method, based on the analysis of more than 350 case histories collected from Canadian underground mines, accounts for the key factors influencing open stope design. Information about the rock mass strength and structure, the stresses around the opening and the size, shape and orientation of the opening is used to determine whether the stope will be stable without support, stable with support, or unstable even if supported. The method also suggests ranges of cablebolt density when the design is in the realm of 'stable with support'.

14.2 The Stability Graph method

The design procedure is based upon the calculation of two factors, N' , the modified stability number which represents the ability of the rock mass to stand up under a given stress condition, and S , the shape factor or hydraulic radius which accounts for the stope size and shape.

14.2.1 The stability number, N'

The stability number, N' , is defined as

$$N' = Q' \times A \times B \times C \quad (14.1)$$

where

- Q' is the modified Q Tunnelling Quality Index
- A is the rock stress factor
- B is the joint orientation adjustment factor
- C is the gravity adjustment factor

The modified Tunnelling Quality Index, Q' , is calculated from the results of structural mapping of the rock mass in exactly the same way as the standard NGI rock mass classification, except that the stress reduction factor SRF is set to 1.00. The system has not been applied in conditions with significant groundwater, so the joint water reduction factor J_w is commonly 1.0. This process is identical to that used earlier in this book for estimating the strength of jointed rock masses (see Equation 8.18 on page 97).

The rock stress factor, A , reflects the stresses acting on the free surfaces of open stopes at depth. This factor is determined from the unconfined compressive strength of the intact rock and the stress acting parallel to the exposed face of the stope under consideration. The intact rock strength can be determined from laboratory testing of the rock or from estimates such as those discussed in Chapter 8. The induced compressive stress is found from numerical modelling or

estimated from published stress distributions such as those in Hoek and Brown (1980a), using measured or assumed in situ stress values. The rock stress factor, A , is then determined from σ_c/σ_1 , the ratio of the intact rock strength to the induced compressive stress on the opening boundary:

$$\begin{aligned} \text{for } \sigma_c/\sigma_1 < 2 : A &= 0.1 \\ \text{for } 2 < \sigma_c/\sigma_1 < 10 : A &= 0.1125 (\sigma_c/\sigma_1) - 0.125 \\ \text{and for } \sigma_c/\sigma_1 > 10 : A &= 1.0 \end{aligned} \quad (14.2)$$

A plot of the rock stress factor A , for different values σ_c/σ_1 is given in Figure 14.1.

The joint orientation adjustment factor, B , accounts for the influence of joints on the stability of the stope faces. Most cases of structurally controlled failure occur along critical joints which form a shallow angle with the free surface. The shallower the angle between the discontinuity and the surface, the easier it is for the bridge of intact rock, shown in Figure 14.2, to be broken by blasting, stress or by another joint set. When the angle θ approaches zero, a slight strength increase occurs since the jointed rock blocks act as a beam. The influence of the critical joint on the stability of the excavation surface is highest when the strike is parallel to the free surface, and smallest when the planes are at right angles to one another. The factor, B , which depends on the difference between the orientation of the critical joint and each face of the stope, can be found from the chart reproduced in Figure 14.3.

The final factor, C , is an adjustment for the effects of gravity. Failure can occur from the roof by gravity induced falls or, from the stope walls, by slabbing or sliding.

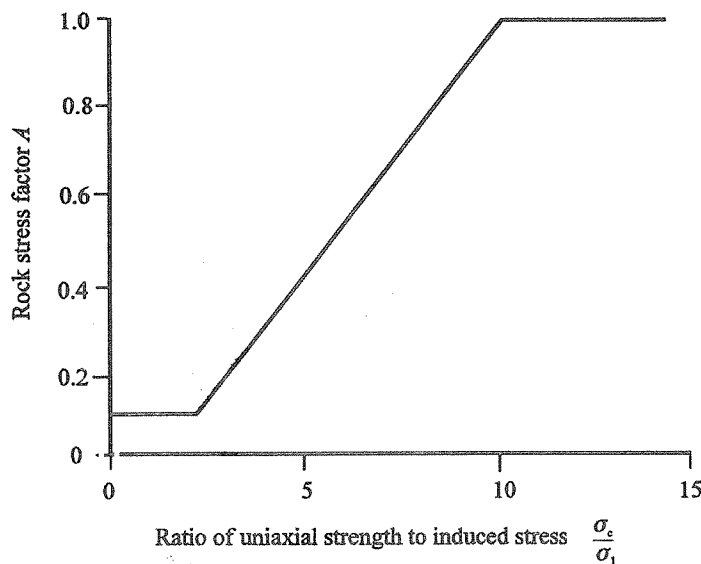


Figure 14.1: Rock stress factor A for different values of σ_c/σ_1

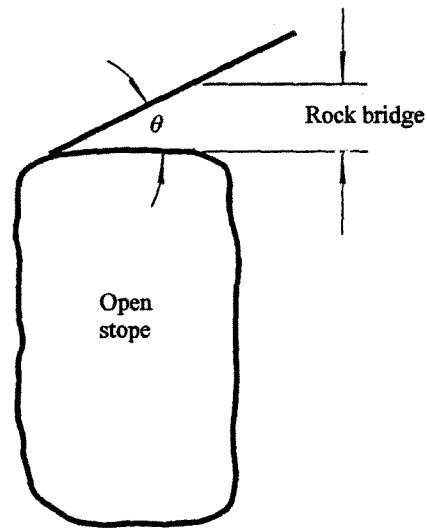


Figure 14.2: Critical joint orientation with respect to the opening surface (After Potvin, 1988).

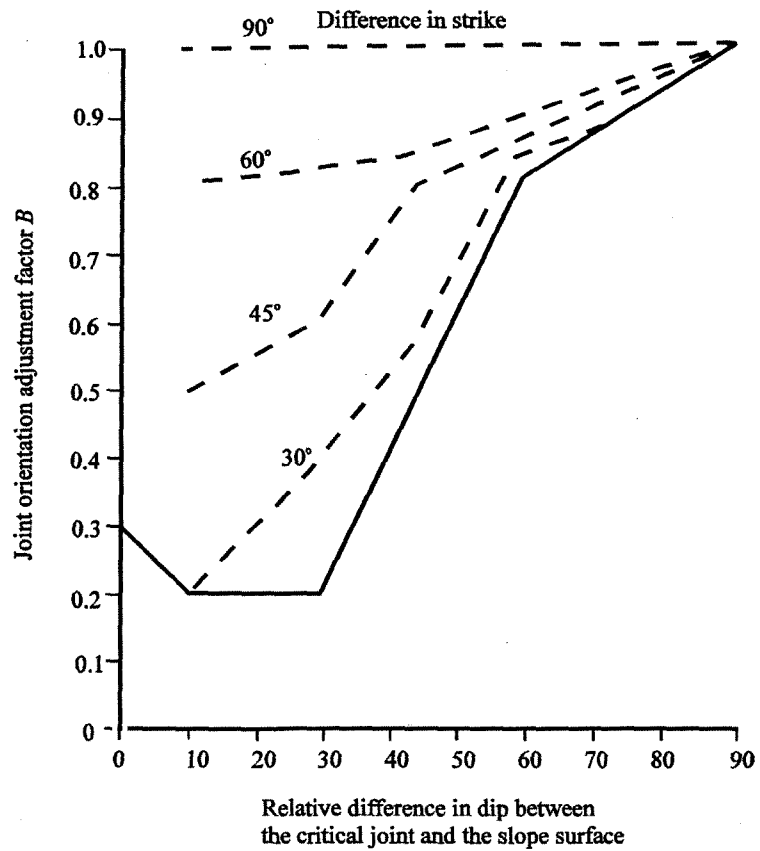


Figure 14.3: Adjustment factor, B , accounting for the orientation of the joint with respect to the stope surface (After Potvin, 1988).

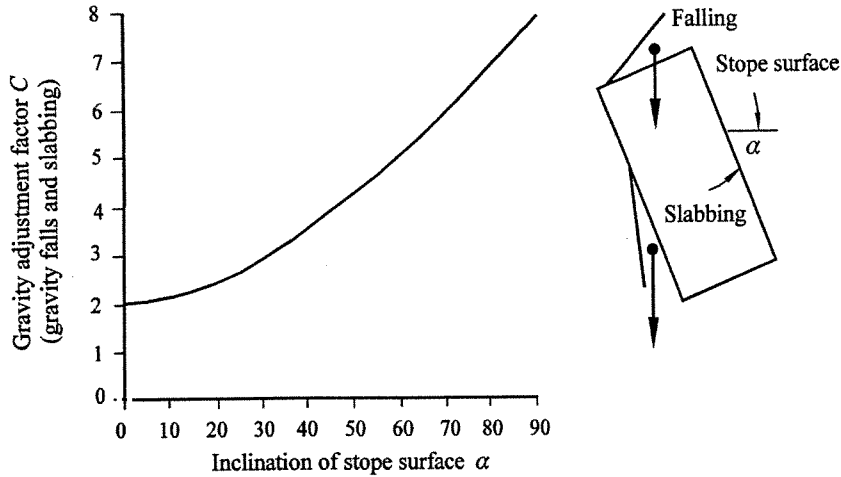


Figure 14.4: Gravity adjustment factor C for gravity falls and slabbing. After Potvin (1988).

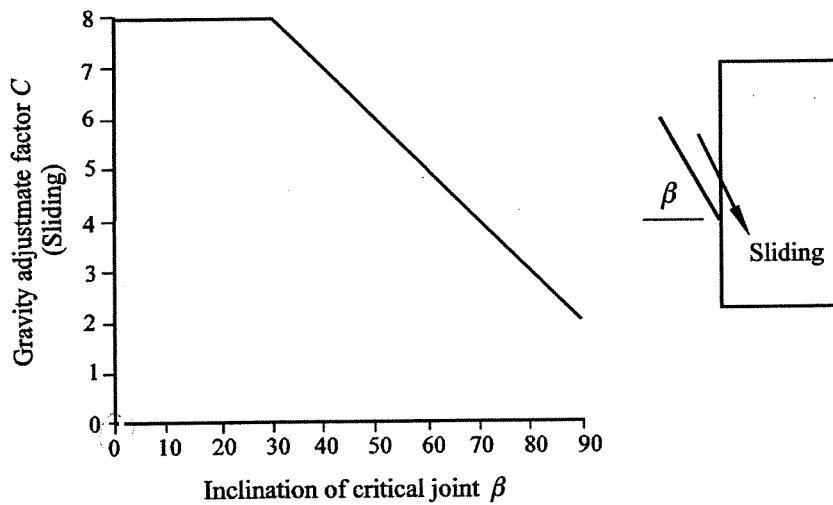


Figure 14.5: Gravity adjustment factor C for sliding failure modes. After Potvin (1988).

Potvin (1988) suggested that both gravity induced failure and slabbing failure depend on the inclination of the slope surface α . The factor C for these cases can be calculated from the relationship, $C = 8 - 6 \cos \alpha$, or determined from the chart plotted in Figure 14.4. This factor has a maximum value of 8 for vertical walls and a minimum value of 2 for horizontal slope backs.

Sliding failure will depend on the inclination β of the critical joint, and the adjustment factor C is given in Figure 14.5.

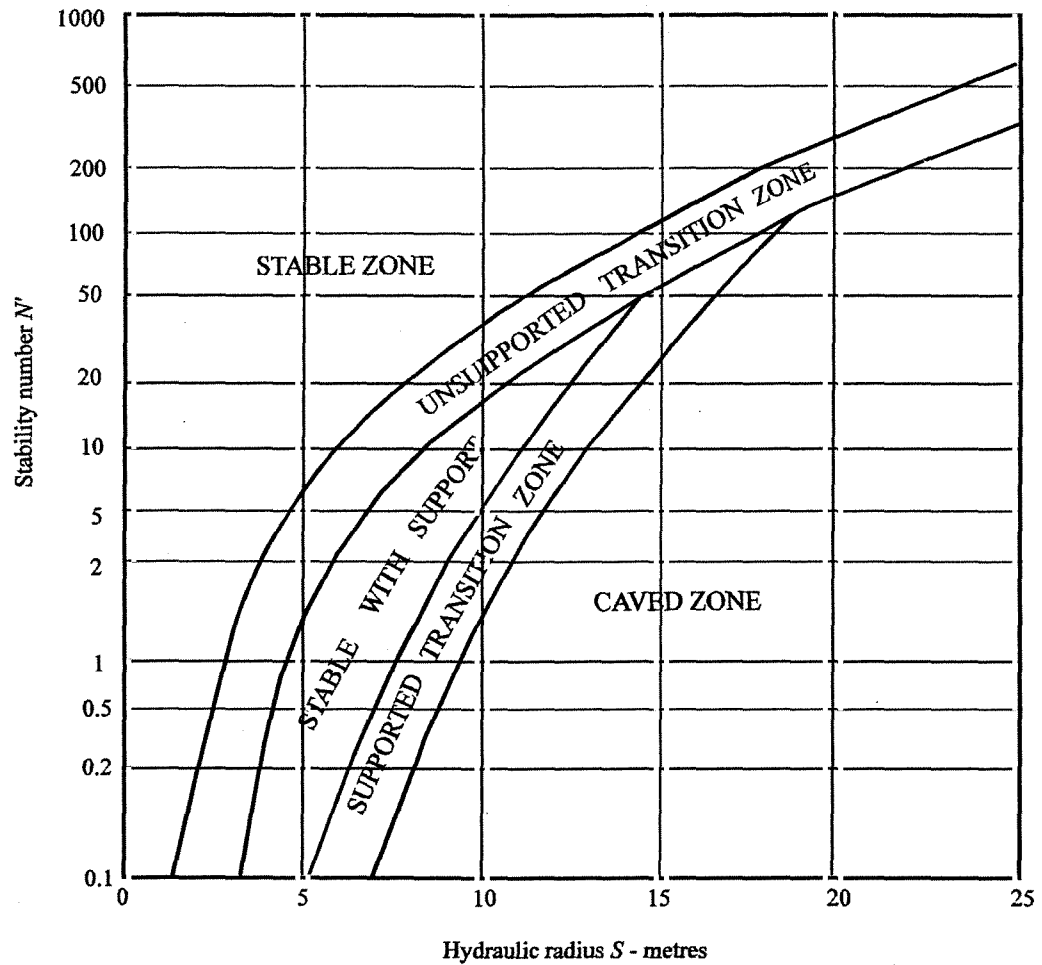


Figure 14.6: Stability graph showing zones of stable ground, caving ground and ground requiring support. After Potvin (1988), modified by Nickson (1992).

14.2.2 The shape factor, S

The hydraulic radius, or shape factor, for the slope surface under consideration, is calculated as follows:

$$S = \frac{\text{Cross sectional area of surface analysed}}{\text{Perimeter of surface analysed}} \quad (14.3)$$

14.2.3 The stability graph

Using the values of N' , the stability number, and S , the hydraulic radius, the stability of the slope can be estimated from Figure 14.6. This figure represents the performance of open slopes observed in many Canadian mines, as tabulated and analysed by Potvin (1988) and updated by Nickson (1992).